Excluded Volume as a Determinant of Macromolecular Structure and Reactivity

ALLEN P. MINTON, *Laboratory of Biochemical Pharmacology, National Institute of Arthritis, Metabolism and Digestive Diseases, National Institutes of Health, Bethesda, Maryland 20205*

Synopsis

The effect of excluded volume on the thermodynamic activity of globular macromolecules and macromolecular complexes in solution is studied in the hard-particle approximation. Activity coefficients are calculated as a function of the fraction of total volume occupied by macromolecules using relations obtained from scaled particle and lattice models. Significant and readily observable effects are predicted to occur as the fraction of volume occupied by globular macromolecules increases, including the following: (i) Compact quasi-spherical macromolecular conformations become increasingly energetically favored over extended anisometric conformations. (ii) Self- and heteroassociation processes are enhanced, particularly those leading to the formation of compact quasi-spherical aggregates. (iii) Depending upon the details of the reaction mechanism, the rate of an enzyme-catalyzed reaction may monotonically decrease, go through a maximum, or exhibit more complex behavior. A given degree of volume occupancy by larger macromolecules is predicted to have less effect on the structure and self-association of smaller macromolecules than the same degree of volume occupancy by smaller macromolecules has on the structure and self-association of larger macromolecules.

INTRODUCTION

The kinetics and equilibria of biochemical reactions are typically studied in solutions in which all macromolecular species are dilute. Many physiological media, however, have substantial macromolecular content. For example, protein comprises about 5% (by weight) of lymph, about 9% of blood plasma, and about 35% of hemolysate.[1] A medium such as cytosol may contain no single macromolecular species at high concentration, yet taken together the mobile macromolecular species occupy a substantial volume fraction of the medium. All of these media may be generally described as *volume-occupied*. We shall use the term *concentrated* in a more restricted sense to describe a medium in which the particular species of interest is (or are) present at high concentration.

The degree to which a medium is volume-occupied may affect biochemical equilibria and kinetics in a variety of ways, due to the many types of interactions which can exist between macromolecules. The purpose of the present work is to demonstrate that even in the absence of direct interactions between macromolecular species, the volume from which macromolecules are excluded by other macromolecules can have a profound

Biopolymers, Vol. 20, 2093–2120 (1981)
 CCC 0006-3525/81/102093-28$02.80

effect on their tertiary or quaternary structures, their state of aggregation, and the kinetics of enzyme-catalyzed reactions. We shall show that at levels of volume-occupancy comparable to those found in physiological media, excluded-volume effects can have energetic consequences equal to or greater than those attributed to intramolecular electrostatic and hydrophobic interactions.

A brief model-independent treatment of the effect of nonideal behavior on thermodynamic equilibria, and by extension (via transition-state theory) on kinetics, is presented below. Two approximate methods used to calculate the effect of excluded volume on thermodynamic activity are described and the effect of excluded volume on conformational equilibria is treated. The effects of excluded volume on macromolecular self-association and on the kinetics of model enzyme-catalyzed reactions, are discussed. Possible biological ramifications of the excluded-volume effects are suggested.

MODEL-INDEPENDENT RELATIONS

Equilibrium

Consider a system containing N molecular species in thermodynamic equilibrium as indicated in the following scheme:

$$n_1X_1 + n_2X_2 + \cdots + n_jX_j \rightleftharpoons n_{j+1}X_{j+1} + n_{j+2}X_{j+2} + \cdots + n_NX_N \tag{1}$$

where n_i represents the stoichiometric coefficient of species X_i. We may generally write the chemical potential μ_i of species X_i as

$$\mu_i = \mu_i^0 + RT \ln a_i = \mu_i^0 + RT \ln \gamma_i c_i \tag{2}$$

where μ_i^0 is the ideal standard state chemical potential of X_i, R the molar gas constant, T the absolute temperature, and a_i, γ_i, and c_i the activity, activity coefficient, and concentration of species X_i, respectively. The ideal standard state of species X_i is defined to be a solution of X_i at unit concentration in which all interactions between solute molecules have been conceptually suppressed ($\gamma_i = 1$). Such a standard state is the solution equivalent of an ideal gas. In the limit of infinite dilution of all species, $\gamma_i \rightarrow 1$ for all i. Thus, we may speak of $\mu_i^0 + RT \ln c_i$ as the ideal part of the chemical potential, μ_i^I, and $RT \ln \gamma_i$ as the nonideal part, μ_i^{NI}.

At equilibrium,

$$\sum_{i=1}^{j} n_i\mu_i = \sum_{i=j+1}^{N} n_i\mu_i \tag{3}$$

Combining Eqs. (2) and (3) and rearranging, we obtain the following expression for the ideal standard state free energy charge ΔG_I^0:

$$\Delta G_I^0 \equiv \sum_{i=j+1}^{N} n_i\mu_i^0 - \sum_{i=1}^{j} n_i\mu_i^0 = -RT \ln K_c + RT \ln \Gamma \tag{4}$$

Here, K_c is an apparent equilibrium constant defined as

$$\prod_{i=j+1}^{N} c_i^{n_i} \Big/ \prod_{i=1}^{j} c_i^{n_i}$$

and Γ is a nonideal correction factor defined as

$$\prod_{i=1}^{j} \gamma_i^{n_i} \Big/ \prod_{i=j+1}^{N} \gamma_i^{n_i}$$

Equation (4) shows that the ideal standard state free-energy change may be conveniently expressed as the difference between a total standard state free-energy change $\Delta G_T^0 \equiv -RT \ln K_c$ and a nonideal contribution $\Delta G_{NI}^0 \equiv -RT \ln \Gamma$. Equation (4) may be rewritten in the form

$$K_c = \exp(-\Delta G_I^0/RT)\Gamma = K_c^0\Gamma \tag{5}$$

We shall subsequently demonstrate that because of excluded-volume effects, the γ_i, and hence Γ and K_c, are functions of the concentrations of all species present in the system, not just the N species participating in the equilibrium scheme (1).

Kinetics

According to transition-state theory of reaction rates, a simple bimolecular reaction may be depicted as

$$A + B \rightarrow (AB)^* \rightarrow \text{products} \tag{6}$$

where $(AB)^*$ represents the activated complex or transition state. Through a procedure which is entirely analogous to that shown above for the equilibrium relations (see, for example, Chap. 5 of Ref. 2), it may be readily shown that the forward rate constant of reaction (6), k, may be given by

$$k = k_0\Gamma^* \tag{7}$$

where Γ^* is a nonideal correction factor defined as $\gamma_A\gamma_B/\gamma_{(AB)^*}$. As in the equilibrium case, we shall observe that γ_A, γ_B, and $\gamma_{(AB)^*}$, and hence Γ^* and k, are functions of the concentrations of all species present, not just those of the reactants.

APPROXIMATE METHODS FOR CALCULATING ACTIVITY COEFFICIENTS

The concentration dependence of thermodynamic and hydrodynamic properties of solutions of hemoglobin and mixtures of hemoglobin and other globular proteins at moderate ionic strength may be quantitatively accounted for if it is assumed that the proteins may be represented by quasi-spherical hard particles of molecular dimensions with no long-range interactions between particles.[3-5] Provided that the salt concentration is sufficiently high (as it would be expected to be in a biological medium),

the electrostatic interactions at neutral pH, like the hydrophobic interactions, are ordinarily of sufficiently short range that their contributions to the nonideal part of the chemical potential of a macromolecule in solution will be negligible relative to the contribution of excluded volume. However, short-range electrostatic and hydrophobic interactions play an important role in determining the standard state chemical potential of any macromolecule or macromolecular aggregate, and hence the value of K_c^0. In the present treatment we shall adopt the hard-particle approximation for the purpose of calculating the nonideal part of the chemical potential of globular macromolecules and their aggregates in solution.

An exact theory for the calculation of the chemical potential of hard particles is available only for two special cases: (1) all particles are spherical and of equal size, and (2) mixtures of particles of different shapes and sizes at low number density (initial deviations from ideal behavior). In order to calculate the chemical potential of hard particles in mixtures of differently sized and shaped particles at higher number densities, it is necessary to employ approximate methods. In the present work we employ two approximate theories, each with different capabilities and limitations, in a complementary manner.

The scaled particle theory for fluid mixtures of Lebowitz et al.[6] as extended by Gibbons[7] provides a prescription for the calculation of the nonideal part of the chemical potential of a hard convex particles (i.e., sphere, cube, right circular cylinder, tetrahedron, ellipsoid of rotation) in an environment of hard particles of similar shape and arbitrary size (Appendix A). Values of the pressure calculated using the scaled particle equation of state for binary mixtures of hard spheres agree to within a few percent with the results of Monte Carlo computer simulations.[6] This finding lends confidence in the significance of results obtained using the scaled particle expression for chemical potential.

A lattice theory has been formulated (Appendix B) which provides a prescription for the activity coefficient of any hard particle which may be represented by rectangular parallelopiped (i.e., a cube, rod of square of rectangular cross section, square or rectangular plate) in an environment of cubes of arbitrary size. In the lattice treatment the planar surfaces of the particles are, for the purposes of simplicity in calculation, artificially constrained to be either parallel or perpendicular to each other. As a result of this constraint, the excluded volume and activity coefficients calculated using the lattice theory are less than the corresponding quantities calculated from a theory, such as the scaled particle theory, which allows arbitrary orientations of particles with respect to one another. However, the lattice theory is used because it permits the calculation of chemical potentials of particles in an environment of differently shaped particles, which the scaled particle theory does not. One can partially correct for the underestimate of activity coefficients in the lattice theory by calibrating it against the scaled particle theory as described in Appendix C.

In subsequent sections we shall present the results of calculations of the

dependence of thermodynamic quantities on the fraction of solution volume occupied by macromolecular solute(s) or, equivalently, the fraction of suspension volume occupied by hard particles representing solute(s). The fractional occupancy, ϕ, is defined to be $\Sigma_i n_i v_i$, where n_i is the number density of particles of species i, and v_i is the volume of a single particle of species i. Unless specified otherwise, the v_i are fixed within the context of a particular calculation; changes in ϕ therefore reflect changes in the number density of particles. This convention enables a direct comparison to be made between the results of calculations and experimental results in which the fractional occupancy of a solution is altered by increasing or decreasing the concentration of a macromolecular solute, the partial specific volume of which is relatively constant.

ISOVOLUMIC CHANGES IN MACROMOLECULAR CONFORMATION (SHAPE)

The volume excluded by a globular macromolecule is dependent both on its size and shape. The term shape is used here to denote the gross outline of the particle at low resolution, neglecting fine indentations and/or projections associated with individual side chains. The shape of a protein may be altered without substantial change in molecular volume by a change in the folding of an individual polypeptide chain (tertiary structure) or the mode of association of polypeptide subunits (quaternary structure) or both. In this section we demonstrate that under appropriate conditions, excluded volume can induce isovolumic changes of macromolecular shape.

Solutions of a Single Macromolecular Species (Homogeneous Suspension of Equivalent Particles)

The value of μ^{NI}/RT (or $\ln \gamma$) calculated using scaled particle theory for suspensions of particles of equal volume and various shapes is plotted as a function of the fractional occupancy ϕ in Fig. 1. The values calculated are independent of particle size so long as particle volume is much smaller than the unit volume used for calculating the number density of particles. For a constant fraction of occupied volume, the value of μ^{NI} increases in the following order of particle shapes: sphere < cylinder [length/diameter $(L/D) = 1$] < cube $\simeq$ cylinder $(L/D = 1/3)$ < cylinder $(L/D = 3)$ < regular tetrahedron. Thus we see that rounded, isometric particles have smaller excluded volume than either anisometric particles (rod, plate) or isometric particles with projecting vertices (cube, tetrahedron).

Let us postulate the following conformational equilibrium:

$$\text{nonspherical particle} \rightleftarrows \underset{\text{(equal volume)}}{\text{sphere}} \qquad (8)$$

with equilibrium constant K_c. The dependence of the nonideal contribution to the free-energy change of this reaction (ΔG^0_{NI}) on the fraction of

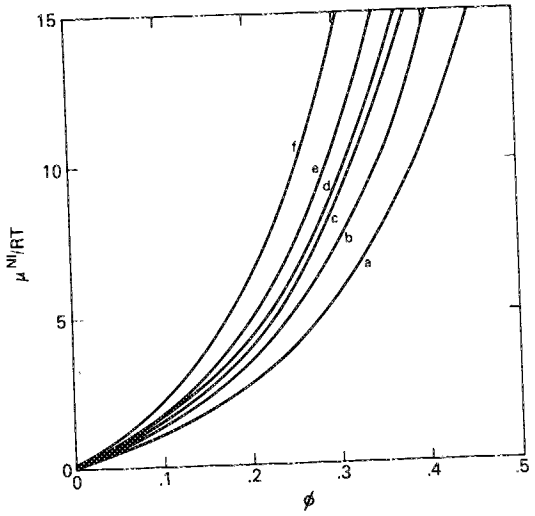

Fig. 1. Nonideal contribution to the chemical potential of variously shaped hard particles in homogeneous suspension, plotted as a function of ϕ, the fraction of volume occupied by the particles: (a) sphere; (b) right circular cylinder, $L/D = 1/1$; (c) cube; (d) cylinder, $L/D = 1/3$; (e) cylinder, $L/D = 3/1$; (f) regular tetrahedron.

total volume occupied by particles is plotted in Fig. 2 for several different nonspherical particle shapes. Let us postulate that the conformational equilibrium indicated above is thermodynamically unfavorable in the absence of excluded-volume effects, i.e., $\Delta G_J^0 > 0$. When ϕ becomes suffi-

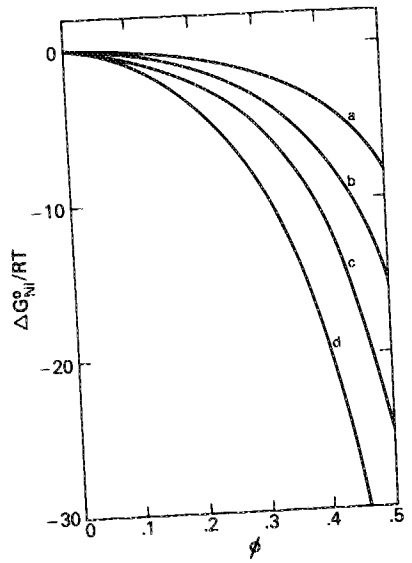

Fig. 2. Nonideal contribution to the standard state free-energy change of reaction (8), plotted as a function of ϕ. Nonspherical particle is (a) right-circular cylinder, $L/D = 1$; (b) cube; (c) cylinder, $L/D = 3$; (d) tetrahedron.

ciently great, the magnitude of ΔG^0_{NI} will exceed that of ΔG^0_I, and the total standard state free-energy charge will become negative. Thus we see that an otherwise unfavorable isovolumic change in tertiary or quaternary structure may be induced by excluded volume when the volume fraction (weight concentration) of solute is sufficiently great.

Solutions Containing Two Macromolecular Species (Heterogeneous Suspension of Equivalent Particles)

In this section the effect of an environment of cubical background particles of different sizes on the chemical potential of a reference particle modeled by a rectangular parallelopiped (PP) is examined. Values of μ^{NI}_{PP}/RT (= ln γ_{PP}) reported were calculated using the lattice model and normalized to the scaled particle results as described in Appendix C.

The chemical potentials of differently shaped PPs of various volume are plotted as functions of the size and volume fraction of background cubes in Fig. 3. The following qualitative trends are noted:

1. For a given PP shape and volume fraction of background cubes, the value of μ^{NI}_{PP} increases with the degree of anisometricity, or deviation from cubic symmetry. The effect is qualitatively similar to that observed in homogeneous systems. The values of μ^{NI}_{PP} for the rodlike and platelike PPs with the same ratio of maximum to minimum dimension are nearly identical.

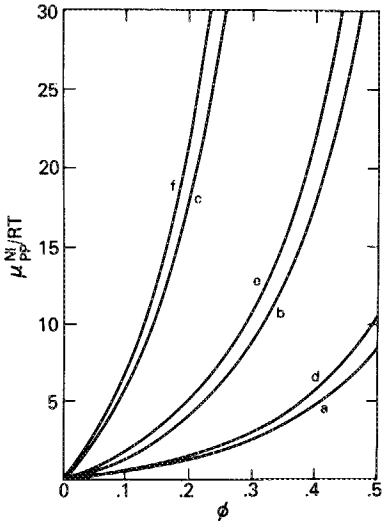

Fig. 3. Nonideal contribution to the chemical potential of a single rectangular parallelopiped of volume v in an environment of cubes of volume v_b, plotted as a function of the fraction of volume occupied by cubes. (a) PP edge ratio = 1:1:1 (cube), $v_b = 10v$; (b) PP same as (a), $v_b = v$; (c) PP same as (a), $v_b = 0.1v$; (d) PP edge ratio = 5:1:1 or 5:5:1, $v_b = 10v$; (e) PP same as (d), $v_b = v$; (f) PP same as (d), $v_b = 0.1v$.

2. For a given PP shape and volume fraction of background cubes, the value of μ_{PP}^{NI} rises sharply as the size of the background cubes decreases. This is because at constant volume fraction, the number density of the cubes increases as their size decreases. At constant number density of background cubes, the value of μ_{PP}^{NI} increases with increasing cube size (data not shown).

The dependence of ΔG_{NI}^0 on ϕ for the conformational equilibrium

$$\text{parallelopiped} \rightleftharpoons \text{cube (equal volume)} \tag{9}$$

is plotted in Fig. 4 for two different PP shapes and three different relative sizes of background cubes. It may be seen that when the volume of a background cube is 10 times that of the reactant PP, the value of $-\Delta G_{NI}^0$ is of order RT or less, even at high volume fractions of environmental cubes. In this instance, the conformational equilibrium is essentially unaffected by the environment. At the other extreme, when the volume of the background cube is 1/10 that of the reference PP, the value of $-\Delta G_{NI}^0$ can become substantial at low volume fractions of environmental particles. These results suggest that in a solution containing a mixture of both large and small macromolecules (for example, proteins ranging from 20,000 to 200,000 in molecular weight), the conformations of the larger species would tend to be influenced more strongly by the overall volume fraction and composition of macromolecules in the solution than would be the conformations of the smaller species.

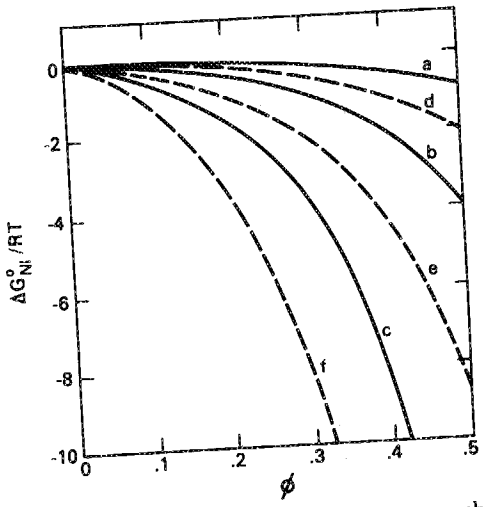

Fig. 4. Nonideal contribution to the standard state free-energy change of reaction (9), plotted as a function of ϕ. (a) PP edge ratio = 3:1:1, $v_b = 10v$; (b) PP same as (a), $v_b = v$; (c) PP same as (a), $v_b = 0.1v$; (d) PP edge ratio = 5:1:1, $v_b = 10v$; (e) PP same as (d), $v_b = v$; (f) PP same as (d), $v_b = 0.1v$.

SELF-ASSOCIATION OF MACROMOLECULES

The effect of nonideal behavior on the concentration dependence of the equilibrium properties of solutions of a single self-associating solute has been treated by several investigators in the limit of initial deviations from ideality.[8–11] These treatments are based on a truncated virial expansion of the logarithm of the activity coefficient, in which terms higher than first order in the concentration of solute are neglected. The theory of self-associating solutes was extended to higher terms in the virial expansion by Hill and Chen.[12]

The present work differs from previous treatments in several of the following particulars: (1) It is assumed that under the conditions of interest, nonideal behavior is due almost entirely to hard-particle interactions between macromolecular species in solution. (2) Nonideal effects are treated independently of intermolecular interactions leading to self-association under ideal conditions. (3) The virial expansion is not employed in the calculation of activity coefficients. (4) Contributions of macromolecular species present in addition to the self-associating species are explicitly considered.

In this section we will model self-association equilibria by the following general scheme:

$$\underset{\text{(volume } v\text{, monomer shape)}}{n \text{ monomers}} \rightleftharpoons \underset{\text{(volume } nv\text{, } n\text{-mer shape)}}{1\ n\text{-mer}} \tag{10}$$

with an equilibrium constant given by Eq. (5). The effect of excluded volume will be manifested in the values of the correction factor, Γ, and the nonideal contribution to the total standard state free energy change, $\Delta G^0_{NI} = -RT \ln \Gamma$.

Self-Association with No Change of Shape

In this subsection we treat the special case of the general reaction indicated above, where $n = 2$, 3, or 4 and the shape of the n-mer is the same as that of the monomer. The dependence of ΔG^0_{NI} on ϕ for a dilute suspension of self-associating cubic particles in an environment of non-self-associating cubic particles of different volumes v_b, as calculated using the lattice model (normalized to the scaled particle model as described in Appendix C), is plotted in Fig. 5.

At constant ϕ, the magnitude of ΔG^0_{NI} increases strongly with increasing n. The value of ΔG^0_{NI} for the reaction

$$\underset{\text{(volume } v\text{)}}{n \text{ cubes}} \rightleftharpoons \underset{\text{(volume } nv\text{)}}{1 \text{ cube}} \tag{11}$$

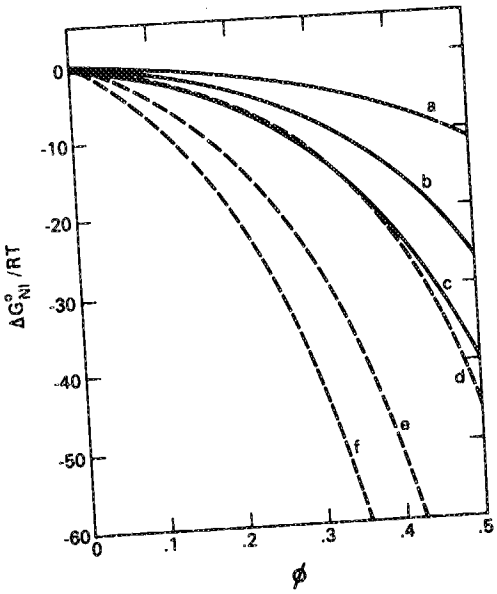

Fig. 5. Nonideal contribution to the standard state free-energy change of reaction (11) plotted as a function of ϕ. (a) $n = 2, v_b = v$; (b) $n = 3, v_b = v$; (c) $n = 4, v_b = v$; (d) $n = 2, v_b = 0.1v$; (e) $n = 3, v_b = 0.1v$; (f) $n = 4, v_b = 0.1v$.

in the homogeneous suspension for a particular value of n and ϕ lies between those calculated for the corresponding heterogeneous suspensions in which $v_b = v$ and $v_b = 0.1v$.

Self-Association with Change of Shape

In this subsection we treat the special cases of the dimerization of rodlike and platelike particles. Consider, first, two alternative modes of dimerization of a rodlike particle:

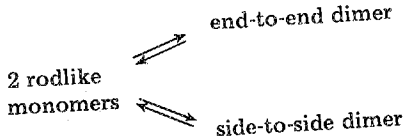

(12)

In the homogeneous system (scaled particle calculation), the rodlike monomer is represented by a right circular cylinder of volume v with $L/D = 2$. The end-to-end dimer is represented by a cylinder of volume $2v$ with $L/D = 4$, and the side-to-side dimer is represented by a cylinder of volume $2v$ with $L/D = 2/\sqrt{2} = 1.414$ (i.e., a cylinder of length equal to that of the monomer with a cross-sectional area twice that of the monomer). These representations are illustrated in Fig. 6(a).

The dependence of ΔG^0_{NI} on ϕ for these two modes of self-association is plotted in Fig. 7. It may be seen that as the fraction of volume occupied

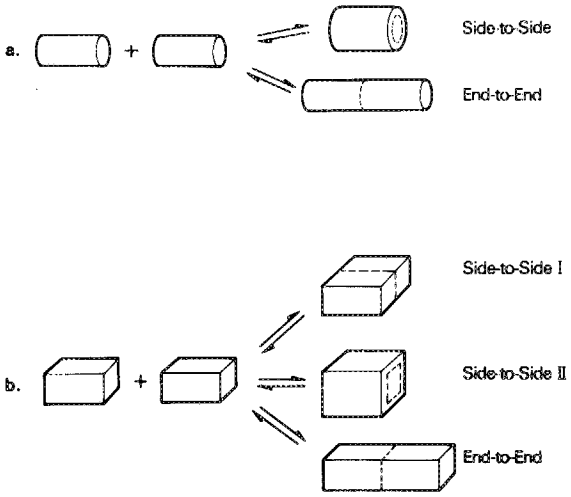

Fig. 6. Schematic representation of modes of dimerization of rodlike particles. (a) Representation as cylinders for scaled particle calculation. (b) Representation as parallelopipeds for lattice calculation.

by particles increases, the value of ΔG^0_{NI} for the side-to-side dimerization becomes increasingly more negative than that for end-to-end dimerization. For example, when $\phi = 0.3$, the value of Γ for side-to-side dimerization is 250 times as great as that for end-to-end dimerization.

In the heterogeneous system (normalized lattice calculation), the rodlike monomer is represented by a PP of volume v with edge ratio 1:1:2, and the end-to-end dimer is represented by a PP of volume $2v$ with edge ratio 1:1:4. The side-to-side dimer is represented in two different ways: (i) as a PP of volume $2v$ with edge ratio 1:2:2 (side-to-side dimer I) and (ii) as a PP of volume $2v$ with edge ratio $\sqrt{2}$:$\sqrt{2}$:2 (side-to-side dimer II). Both side-

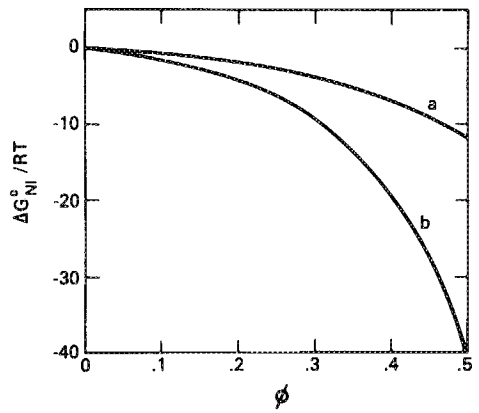

Fig. 7. Nonideal contribution to the standard state free-energy charge of reaction (12) in homogeneous suspension plotted as a function of ϕ for formation of end-to-end dimer (a) and side-to-side dimer (b).

to-side dimers have a length equal to that of the monomer, but dimer I has a rectangular cross section equal to that of two monomers laid side by side, whereas dimer II has a square cross section of area equal to twice that of a monomer. These representations are illustrated in Figure 6(b).

The dependence of ΔG^0_{NI} on the fraction of volume occupied by cubical background particles is plotted for the three alternate modes of self-association and two relative volumes of background cubes in Fig. 8. It may be observed that as in the homogeneous system, volume exclusion favors the formation of side-to-side dimers over formation of end-to-end dimers. While there is a perceptible difference between the values of ΔG^0_{NI} for formation of side-to-side dimers I and II, this difference is small relative to the difference between the values of ΔG^0_{NI} for the end-to-end dimer and either side-to-side dimer, indicating that in this instance, the detailed representation of the shape of the side-to-side dimer is unimportant from a qualitative point of view.

We next consider two alternative modes of dimerization of the platelike particle:

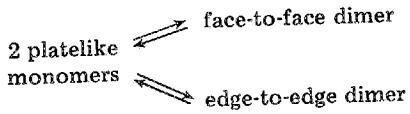

(13)

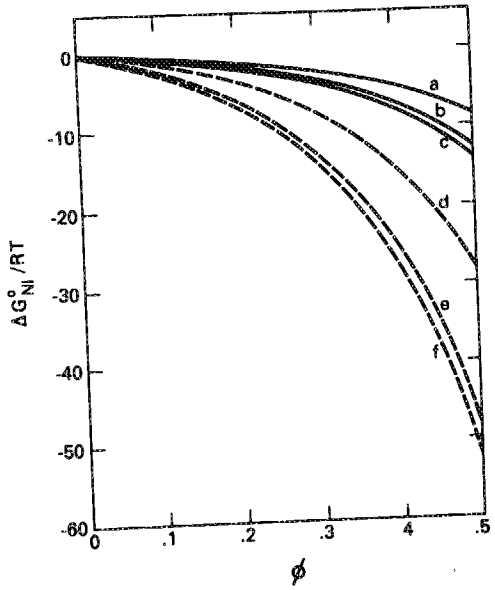

Fig. 8. Nonideal contribution to the standard state free-energy charge of reaction (12) in heterogeneous suspension, plotted as a function of ϕ for formation of end-to-end dimer (a,d), side-to-side dimer I (b,e), and side-to-side dimer II (c,f). Solid curves, $v_b = v$; dashed curves, $v_b = 0.1v$.

As illustrated in Fig. 9(a), for the purpose of a scaled particle calculation on a homogeneous system, the platelike monomer is represented by a right circular cylinder of volume v with $L/D = 0.5$ and the face-to-face dimer by a cylinder of volume $2v$ with $L/D = 1$. The edge-to-edge dimer is represented by a cylinder of volume $2v$ with $L/D = 0.5/\sqrt{2} = 0.3536$ (i.e., a cylinder with the same length and twice the cross-sectional area of the monomer). This particular representation of the edge-to-edge dimer is less realistic than one would like, being too isometric, but it is the best currently available within the context of the scaled particle model. A better representation of the edge-to-edge dimer of platelike particles can be made in the context of the lattice model.

As illustrated in Fig. 9(b), for the purpose of a normalized lattice calculation on a heterogeneous system, the platelike monomer is represented by a PP of volume v with edge ratio 1:2:2, and the face-to-face dimer is represented by a PP of volume $2v$ with edge ratio 2:2:2. The edge-to-edge dimer is represented in two different ways: (i) as a PP of volume $2v$ with edge ratio 1:2:4 (edge-to-edge dimer I) and (ii) as a PP of volume $2v$ with edge ratio $1:\sqrt{8}:\sqrt{8}$ (edge-to-edge dimer II). Both side-to-side dimers have their length (shortest dimension) equal to that of the platelike monomer, but dimer I has a rectangular cross section equal to that of two monomers laid side by side, whereas dimer II has a square cross section of area equal

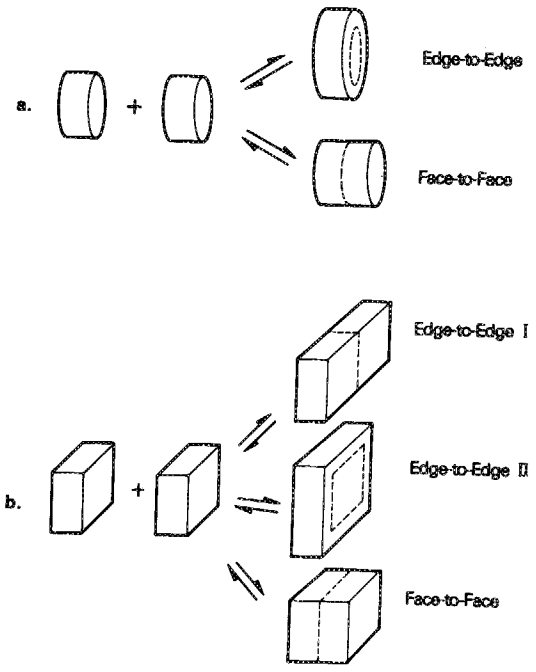

Fig. 9. Schematic representation of modes of dimerization of platelike particles. (a) Representation as cylinders for scaled particle calculation. (b) Representation as parallelopipeds for lattice calculation.

to twice that of monomer. (It may be seen that dimer II is the counterpart in the heterogeneous system calculation of the cylindrical representation of the edge-to-edge dimer in the homogeneous system calculation).

The results of scaled particle and lattice calculations of the dependence of ΔG^0_{NI} on ϕ for reaction (13) may be summarized as follows: The magnitude of ΔG^0_{NI} for a given value of ϕ is qualitatively comparable to that calculated for dimerization of rodlike particles (Figs. 7 and 8). At a given value of ϕ, formation of face-to-face dimers of platelike molecules is energetically favored over the formation of side-to-side dimers by about the same margin as the formation of side-to-side dimers of rodlike molecules is energetically favored over the formation of end-to-end dimers.

Condensation

The formation of a condensed (crystalline, quasi-crystalline) phase may be considered to be self-association in the limit of indefinitely large n. In this limit the thermodynamic activity of the aggregate may be taken to be independent of the size of the aggregate, hence constant at constant temperature and pressure. The activity of monomer in equilibrium with aggregate will likewise be constant at constant temperature and pressure.

If background molecules are added to the system containing dissolved monomer and condensed phase, and if it is stipulated that they are restricted to the solution phase, then background molecules will have no effect on the activity of the condensed phase or on the equilibrium activity of dissolved monomer. But the volume excluded by the background molecules will increase the activity coefficient of the dissolved monomer in equilibrium with aggregate, thereby decreasing its concentration (i.e., the solubility of monomer). Ross and Minton[13] recently treated the case of mixtures of a low-solubility variant of hemoglobin and other highly soluble proteins (background molecules) and derived the following expression for the solubility of the hemoglobin:

$$c_s = c_s^0 \gamma_s^0 / \gamma_s \tag{14}$$

where c_s and c_s^0 are, respectively, the solubilities of monomer in the presence and absence of background molecules, and γ_s and γ_s^0 are, respectively, the activity coefficients of monomer at saturation in the presence and absence of background molecules.

The dependence of the solubility of a sparingly soluble solute (modeled by a cube of volume v) on the volume fraction of background particles (modeled by cubes of volume v_b) is plotted in Fig. 10 for three values of v_b.

RATES OF ENZYME-CATALYZED REACTIONS

The mechanism of an enzyme-catalyzed reaction may be broken down into a series of elementary reaction steps: (a) the binding of substrate(s) to the enzyme, (b) the reaction of enzyme-bound substrate(s) to form en-

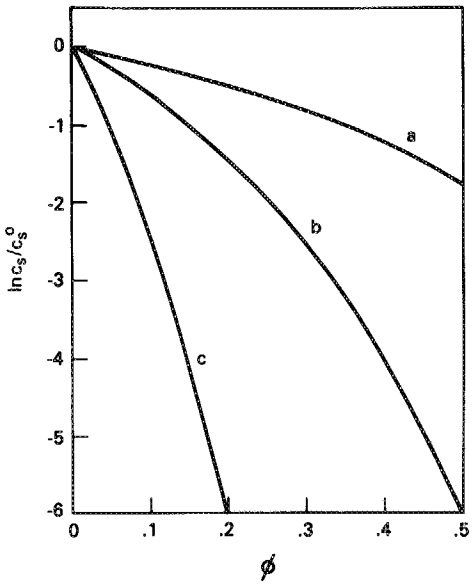

Fig. 10. Solubility of cubic particles as a function of ϕ. (a) $v_b = 10v$; (b) $v_b = V$; (c) $v_b = 0.1v$.

zyme-bound product(s), and (c) the dissociation of product(s) from the enzyme. In principle, any of these steps or even the initial rate of encounter of enzyme and substrate molecules may be rate-limiting. Using a simple enzyme-catalyzed reaction as a prototype, we shall first present the initial rate law appropriate to each of the possible rate-limiting processes. Then we shall examine how excluded volume can affect the values of each of the parameters appearing in the rate laws and the overall rate predicted by each of the rate laws.

The enzyme-catalyzed reaction schematically depicted by

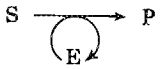

(15)

where S, P, and E are respectively substrate, product and enzyme, may be represented by the following series of elementary reaction steps:

$$\text{(I)} \qquad S + E \underset{k_{-1}}{\overset{k_1}{\rightleftharpoons}} SE \qquad K_1 \equiv k_1/k_{-1}$$

$$\text{(II)} \qquad SE \underset{k_{-2}}{\overset{k_2}{\rightleftharpoons}} PE \qquad K_2 \equiv k_2/k_{-2} \qquad (16)$$

$$\text{(III)} \qquad PE \underset{k_{-3}}{\overset{k_3}{\rightleftharpoons}} P + E \qquad K_3 \equiv k_3/k_{-3}$$

For the purpose of calculating the initial rate laws characterizing the various rate-limiting situations, it will be assumed that the rate constant characterizing the rate-limiting process is much smaller than all other rate constants. It follows that all species preceding the rate-limiting step will be present at steady-state concentrations essentially equal to their equilibrium concentrations and that all species following the rate-limiting step will be present at negligible concentration.

Step I rate limiting:

$$k_1 \ll k_i (i \neq 1);\ [\mathrm{SE}],\ [\mathrm{PE}],\ [\mathrm{P}] \simeq 0$$
$$\text{rate} = k_1[\mathrm{S}][\mathrm{E}] \simeq k_1[\mathrm{S}]E_T \tag{17}$$

where E_T is the total concentration of enzyme present.

Step II rate-limiting (Michaelis-Menten Kinetics):

$$k_2 \ll k_i (i \neq 2);\ [\mathrm{PE}],\ [\mathrm{P}] = 0$$
$$\text{rate} = k_2[\mathrm{SE}] \simeq k_2 K_1[\mathrm{S}][\mathrm{E}]$$
$$= k_2 E_T K_1[\mathrm{S}]/(1 + K_1\mathrm{S}) \tag{18}$$

Step III rate-limiting (quasi-Michaelis-Menten Kinetics):

$$k_3 \ll k_i (i \neq 3);\ [\mathrm{P}] = 0$$
$$\text{rate} = k_3[\mathrm{PE}] \simeq k_3 K_2 K_1[\mathrm{S}][\mathrm{E}]$$
$$= k_3 E_T K_2 K_1[\mathrm{S}]/\{1 + (K_1 + K_2 K_1)[\mathrm{S}]\} \tag{19}$$

In the following subsections we shall evaluate the dependence of the various rate and equilibrium parameters appearing in these rate laws on ϕ, the fraction of solution volume occupied by background molecules. It is reemphasized that background molecules do not interact with substrate, product, or enzyme, except through volume exclusion.

Dependence of E_T on ϕ

There exist at least two ways in which E_T may vary with ϕ. We shall consider each separately.

1. The enzyme may exist in two or more conformations with different enzymic activities, and excluded volume may shift the equilibrium between these conformations so as to alter their relative abundances. As a simple example, consider an enzyme which can exist as a rodlike particle of volume v (modeled by a PP of edge ratio 1:1:5) or as a quasi-spherical particle of equal volume (modeled by a cube). The two conformational states are in rapid dynamic equilibrium, and in the absence of excluded-volume effects, the rodlike conformation is more stable; for the equilibrium

$$\underset{\text{(enzymically inactive)}}{\text{rodlike conformation}} \rightleftarrows \underset{\text{(enzymically active)}}{\text{quasi-spherical conformation}}$$

Let the ideal equilibrium constant for the conformational change, K_c^0, be

0.01. Using the calculated values of ΔG^0_{NI} for this equilibrium, presented in Fig. 4, the fraction of enzyme existing in the quasi-spherical conformation may be calculated as a function of ϕ, the fraction of solution volume occupied by background cubes of volume v. The result of this calculation is that in media where $\phi > 0.3$, the enzyme will exist almost entirely (>95%) in the active (quasi-spherical) conformation, while in media where $\phi < 0.15$, less than 10% of the enzyme will exist in the active conformation. In this example, a dilution of the high volume occupancy (i.e., physiological) medium by a factor of just two can lead to an almost 10-fold loss of specific enzyme activity.

2. The enzyme may self-associate in volume-occupied media, and the catalytic activity of the enzyme may vary with the degree of self-association. As a simple example, let us postulate that an enzyme may exist as either a monomer, represented by a cube of volume v, or as a compact tetramer, represented by a cube of volume $4v$.

$$4 \text{ monomer} \rightleftarrows \text{tetramer}$$

$$K_c = \frac{c_{\text{tetramer}}}{c^4_{\text{monomer}}} \tag{20}$$

Let the ideal equilibrium constant for tetramerization, K^0_c, be $10^{15}M^{-3}$. Using the scaled particle model, the value of K_c for this equilibrium may be calculated as a function of ϕ, the volume fraction of background cubes of volume v_b. The calculated weight fraction of enzyme present as tetramer, at a total enzyme concentration ($c_{\text{monomer}} + 4c_{\text{tetramer}}$) of $10^{-6}M$, is plotted in Fig. 11 as a function of ϕ. If it is assumed that only one of the two states of aggregation is catalytically active, and that all substrates are present at saturating concentrations, then one can see how a relatively

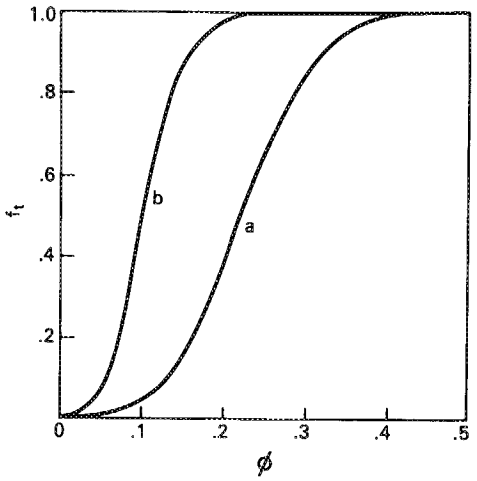

Fig. 11. Fraction of hypothetical enzyme existing as tetramer, f_t, plotted as a function of ϕ. (a) $v_b = v$; (b) $v_b = 0.1v$.

minor change in the dilution of the entire medium can result in a very large change in the concentration of active species, and hence reaction rate.

Dependence of K_i on ϕ

As shown above, the overall equilibrium constant may be written as the products of an ideal equilibrium constant and a nonideal correction:

$$K_1 = K_1^0\Gamma_1, \quad \Gamma_1 = \gamma_S\gamma_E/\gamma_{ES}$$
$$K_2 = K_2^0\Gamma_2, \quad \Gamma_2 = \gamma_{ES}/\gamma_{EP} \tag{21}$$

If S is a macromolecule of volume comparable to that of E, then Γ_1 would be expected to increase rapidly with increasing ϕ. If S is a small molecule, then neither Γ_1 nor Γ_2 would be expected to vary greatly with ϕ unless binding of S or conversion of enzyme-bound S to P was associated with a large conformational change of E.

The following quantitative example will provide an illustration of the possible magnitude of the effect of excluded volume on Γ_1 if S is a macromolecule. We postulate that E and S are approximately the same size and shape, and model the formation of ES by the association of two cubes of volume v to form a PP of volume $2v$ with edge ratio 1:1:2. The dependence of Γ_1 on ϕ, the fraction of volume occupied by background cubes of volume v_b, is plotted in Fig. 12. It may be seen that under certain conditions, the value of K_1 may increase by two or more orders of magnitude at relatively low values of ϕ.

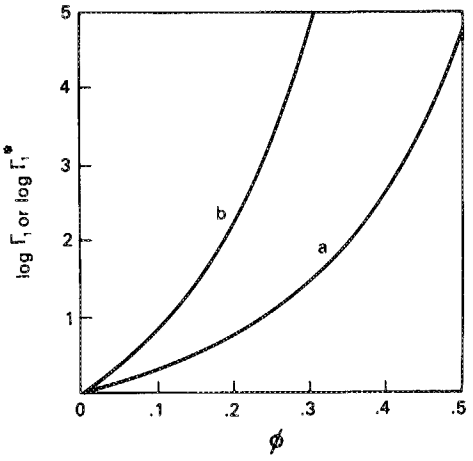

Fig. 12. Nonideal correction factor to equilibrium and rate constants for examples given in text, plotted as a function of ϕ. (a) $v_b = v$; (b) $v_b = 0.1\,v$.

Dependence of k_i on ϕ

As shown above, the rate constants may be written as products of ideal rate constants and nonideal correction factors:

$$\begin{aligned} k_1 &= k_1^0\Gamma_1^*, \quad \Gamma_1^* = \gamma_E\gamma_S/\gamma_{I^*} \\ k_2 &= k_2^0\Gamma_2^*, \quad \Gamma_2^* = \gamma_{ES}/\gamma_{II^*} \\ k_3 &= k_3^0\Gamma_3^*, \quad \Gamma_3^* = \gamma_{EP}/\gamma_{III^*} \end{aligned} \tag{22}$$

where γ_{I^*}, γ_{II^*}, and γ_{III^*} are the respective activity coefficients of the activated complexes for elementary reaction steps I, II, and III. Unless one of these reaction steps entails a large change in the shape of the enzyme–substrate/product complex, we may make the approximation that for any ϕ,

$$\gamma_{I^*} \simeq \gamma_{II^*} \simeq \gamma_{III^*} \simeq \gamma_{ES} \simeq \gamma_{EP} \equiv \gamma_C \tag{23}$$

where the subscript C indicates that the activity coefficient is characteristic of the complex.

According to this approximation, $\Gamma_2^* \simeq \Gamma_3^* \simeq 1$. If S is a small molecule, then $\Gamma_1^* \simeq 1$ as well. However, if S is a macromolecule with volume comparable to that of E, then Γ_1^* may increase substantially with increasing ϕ.

The following quantitative example will provide an illustration of the possible magnitude of the effect of excluded volume on k, if S is a macromolecule. We postulate that E and S are approximately the same size and shape, and are modeled by cubes of volume v. The activated complex leading to formation of ES is assumed to have approximately the same conformation and activity coefficient as ES, which is modeled by a PP of volume $2v$ with edge ratio 1:2:2. Thus, in this example the dependence of Γ_1^* on ϕ will be identical to the dependence of Γ_1 on ϕ, which is plotted in Fig. 12.

The formulation of the rate constant k_1 given in Eq. (22) is only valid so long as the assumptions inherent in the transition-state theory of reaction rates are valid. One of these assumptions is that the rate at which transition-state complexes are formed is great relative to the rate at which they decay to form product(s). If the rate at which molecules of E and S encounter each other in solution is small relative to the intrinsic rate with which activated complex decays to the stable species ES, then the encounter rate will be rate-limiting. Under these conditions transition-state theory is inapplicable, and the reaction rate will be equal to the encounter rate. In Appendix D it is shown that the dependence of encounter rate constant upon ϕ may be approximated by

$$k_e \sim k_e^0 e^{-g\phi} \tag{24}$$

where k_e^0 is the encounter rate constant in the absence of background molecules, and g is a constant whose magnitude is a function of the relative sizes and shapes of enzyme, substrate, and background molecules. Since

the overall rate of the enzyme-catalyzed reaction may not exceed the encounter rate under any conditions, and since the encounter rate decreases monotonically with increasing ϕ, it is clear that, independent of the detailed mechanism of the enzyme-catalyzed reaction, there exists a degree of volume occupancy ϕ^* such that for all $\phi > \phi^*$, the rate of the reaction will decrease monotonically with increasing ϕ.

Dependence of Overall Rate on ϕ

Having considered the effect of volume occupancy on the values of the several parameters appearing in the rate law expressions, we may now proceed to evaluate the effect of volume occupancy on the overall rate for each of the rate-limiting situations listed at the outset of this section. It will be initially assumed that E_T is independent of ϕ; effects due to variation of E_T with ϕ will be considered subsequently.

Step I Rate-Limiting

If $k_1^0 < k_e^0$, then the reaction rate will increase with increasing ϕ until $k_1 \sim k_e$. At this point, the rate will level off, reach a maximum value, and then decrease with increasing ϕ as the encounter between E and S becomes rate-limiting. If $k_1^0 \geq k_e^0$, then the reaction rate will decrease monotonically with increasing ϕ.

Step II Rate-Limiting

When $K_1[\mathrm{S}] \ll 1$, the rate will increase with increasing ϕ due to the increase of K_1 with ϕ. The rate will attain a limiting value of K_2E_T when $K_1[\mathrm{S}] \gg 1$. So long as step II is rate-limiting and E_T is constant, further increases in ϕ would not be expected to affect the rate greatly. Note that the limiting rate may be attained in the absence of background molecules simply by increasing the concentration of S. Laurent[14] has previously considered this case (Michaelis-Menten kinetics) and arrived at the same qualitative conclusions.

Step III Rate-Limiting

This case is almost identical to the case where Step II is rate-limiting. When $K_1K_2[\mathrm{S}] \ll 1$, the rate will increase with increasing ϕ due to the increase of K_1 with ϕ. The rate will attain a limiting value of k_3E_T when $K_1K_2[\mathrm{S}] \gg 1$. So long as step II is rate-limiting and E_T is constant, further increases in ϕ would not be expected to affect the rate greatly. As noted above for the previous case, the maximum rate may be attained in the absence of background molecules by sufficiently increasing the concentration of substrate.

It should be emphasized that the maximum rate predicted by either Eqs.

(18) or (19) may not necessarily be attained with increasing ϕ. The possibility exists that at a value of ϕ such that $K_1[S]$ (or $K_1K_2[S]$) $\gg 1$, the encounter rate rather than step II or III will be rate-limiting.

Summarizing the above, it is found that for constant E_T, an increase in ϕ may lead either to a monotonic decrease in rate or an increase followed by a decrease in rate. These effects may be superimposed on effects due to changes in E_T with increasing ϕ, such as those discussed above. If, for example, the specific catalytic activity of a particular oligomeric species of self-associating enzyme is decreasing with ϕ, but its concentration is increasing with ϕ, then the overall reaction rate could increase monotonically, decrease monotonically, or go through a minimum and/or maximum with increasing ϕ, depending on the values of the rate and equilibrium parameters characterizing the system.

DISCUSSION

We may qualitatively summarize the results presented in the preceding three sections as follows:

1. As volume occupancy increases, compact quasi-spherical macromolecular conformations become increasingly energetically favored over extended anisometric conformations.
2. As volume occupancy increases, self-association processes are enhanced, particularly those leading to the formation of compact, quasi-spherical aggregates.
3. A given degree of volume occupancy by larger macromolecules has less effect on the structure and self-association of smaller macromolecules than the same degree of volume occupancy by smaller macromolecules has on the structure and self-association of larger macromolecules.
4. As volume occupancy increases, the rate of an enzyme-catalyzed reaction may monotonically decrease, go through a maximum, or exhibit more complex behavior.

Model calculations have indicated that for some types of reactions or structural changes, the excluded-volume contribution to the standard state free-energy change may amount to several tens of kcal/mol under conditions of high volume occupancy. Thus, the effect of excluded volume on reaction rates or equilibria should be readily observable if the experimental system is properly chosen.

Laurent[14] and Jancsik et al.[15] have studied the effect of added water-soluble polymers on enzyme kinetics, and Laurent and Obrink[16,17] have studied the effect of added polymers on the rotational diffusion of proteins. While excluded volume must play a significant role in the observed effects, the use of random-coil polymers (as opposed to globular proteins) as space-filling molecules renders a quantitative theoretical analysis prohibitively difficult.

The only protein solutions which have been quantitatively studied at concentrations in excess of 10 g/dl are those of the hemoglobins and serum

albumin. It has been shown that the solubility of deoxy sickle hemoglobin (HbS) decreases on addition of other proteins which do not coprecipitate with HbS.[18-20] The dependence of HbS solubility on the concentration of the other protein may be quantitatively accounted for on the basis of excluded-volume effects as discussed above.[13,20]

In an effort to test some of the qualitative predictions enumerated above, a number of parallel experimental investigations have been initiated. The major results of these investigations, which will be reported elsewhere, are summarized as follows:

1. Myoglobin, which behaves as a monomer in dilute solution, appears to self-associate to form dimers and/or higher oligomers at concentrations in excess of 20 g/dl (A. P. Minton and M. S. Lewis, submitted for publication).

2. A fluorescent derivative of myoglobin at low concentration (<0.2 g/dl) appears to self-associate to dimers in the presence of concentrations of other globular proteins in excess of 20 g/dl.[21]

3. The enzyme glyceraldehyde-3-phosphate dehydrogenase (GAPD) consists of four identical subunits which reversibly dissociate at high dilution.[22,23] The specific activity of the enzyme decreases with increasing enzyme concentration in a manner which suggests that the enzyme activity varies with the degree of subunit association.[15] We have measured the dependence of GAPD activity on GAPD concentration in the absence and presence of 18 g/dl ribonuclease A and measured the dependence of GAPD activity at fixed GAPD concentration on the concentration of three added proteins (ribonuclease A, β-lactoglobulin, and bovine serum albumin). All of our results may be semiquantitatively accounted for by a simple model, containing only a single adjustable parameter. According to this model, under the conditions of our experiments, GAPD exists primarily as an equilibrium mixture of monomeric subunits of high enzymatic activity and tetramers of approximately 30-fold lower activity. The addition of other globular proteins shifts the monomer–tetramer equilibrium in the direction of tetramer, as proposed above, without substantially affecting the specific activity of either monomer or tetramer.[24]

Although the hard-particle representation of protein solutions is obviously oversimplified, and although the scaled particle and lattice theories used here to calculate chemical potentials and activity coefficients are approximate, all of the experimental results obtained to date are in at least qualitative accord with the predictions of the model calculations presented here.

Two implications of the results presented in this report are evident: (1) In high-occupancy (physiological) media, excluded-volume effects provide a contribution to the overall balance of forces determining the tertiary and quaternary structures and the state of association of globular macromolecules which may be energetically comparable to those of the more frequently invoked electrostatic and hydrophobic interactions. (2) Extreme caution must be exercised when attempting to apply the results of structural and

functional studies on biological macromolecules in dilute solution to physiological systems. The approximate theory presented here provides a means of estimating corrections which will undoubtedly have to be applied to the results of dilute solution studies in order to obtain results which are meaningful in a physiologic context.

APPENDIX A

Selected Results of Scaled Particle Theory for Mixtures of Hard Convex Particles

Gibbons[7,25] has generalized the scaled particle theory for hard-sphere mixtures[6] to the case of mixtures of convex particles of different sizes but similar shapes. In this appendix we present his main results using a simplified notation.

Let R represent the characteristic linear dimension of a particle, for example the radius of a sphere or the side of a cube. The average radius, the surface area, and the volume of the particle may be expressed respectively as aR, bR^2, and cR^3, where a, b, and c are constants determined by the shape (not the size) of the particle. These constants have been tabulated for several particle shapes in Table I of Gibbons.[25] (There is a misprint in one entry in this table. The correct value for a for a regular tetrahedron is $(3\tan^{-1}\sqrt{2})/2\pi$. Also, for a right circular cylinder of radius R and length to diameter ratio L, one calculates $a = 4(\pi + 2L)$, $b = (2 + 4L)\pi$, $c = 2\pi L$.)

Consider a mixture of M classes of similarly shaped particles. The ith class is characterized by the number density d_i and characteristic linear dimension R_i. The values of a, b, and c are the same for all classes of particles, since they have the same shape. The nonideal part of the chemical potential of the jth class is given by

$$\frac{\mu_j^{NI}}{RT} = -\ln(1-Y) + \left(\frac{aB}{1-Y}\right)R_j + \left(\frac{bA + 0.5a^2B^2}{(1-Y)^2}\right)R_j^2 + c\left(\frac{d}{1-Y} + \frac{B^2C}{3(1-Y)^3} + \frac{AB}{(1-Y)^2}\right)R_j^3 \quad \text{(A1)}$$

where

$$d \equiv \sum_{i=1}^{M} d_i$$

$$A \equiv a\sum_{i=1}^{M} R_i d_i, \quad B \equiv b\sum_{i=1}^{M} R_i^2 d_i, \quad C = a^2\sum_{i=1}^{M} R_i^2 d_i$$

$$Y = c\sum_{i=1}^{M} R_i^3 d_i$$

It will be noted that Y is equal to the total volume fraction occupied by particles. In the present treatment this is equivalent to ϕ, the volume fraction of solution occupied by globular macromolecules.

APPENDIX B

Lattice Model for Calculation of the Chemical Potential of a Hard Rectangular Parallelopiped in an Environment of Hard Cubes

Consider a system of volume V containing N hard cubes of side b and Z hard rectangular parallelopipeds (PPs) of sides a_1, a_2, a_3. Let the system be extremely dilute in PPs, i.e., $Za_1a_2a_3/V \simeq 0$. In the hard-particle approximation, the energy of the system is taken to be zero, so that the Helmholtz free energy, A, is just $-TS$, where T is the absolute temperature and S the entropy of the system. Then, the chemical potential of a PP is

$$\mu_{PP} = \left(\frac{\partial A}{\partial Z}\right)_N = -T\left(\frac{\partial S}{\partial Z}\right)_N \tag{B1}$$

In order to calculate S and $(\partial S/\partial Z)_N$, we employ a lattice model.[26] Consider a cubic lattice of M sites, where $M \propto V$. Particles are constructed on the lattice by filling adjacent lattice sites. For example, a cube of side b is represented by a cubic block of $b \times b \times b$ filled lattice sites. The entropy of the lattice model is given by

$$S^{LM} = R \ln g(Z,N) \tag{B2}$$

where $g(Z,N)$ is the number of distinguishable conformations of the system containing Z PPs and N cubes. The chemical potential of a PP in this model is then

$$\mu_{PP} = -RT\left(\frac{\partial \ln g(Z,N)}{\partial Z}\right)_N \tag{B3}$$

Let ν_j be the number of ways of putting one PP into a system containing N cubes and $j-1$ PPs. Then,

$$g(Z,N) = \frac{1}{Z!}\prod_{j=0}^{Z-1}\nu_j \times g(0,N) \tag{B4}$$

where the factor $1/Z!$ takes into account the indistinguishability of the PPs. Since the PPs are too dilute to interact with one another, $\nu_j \simeq \nu_1$ for $0 \leq j \leq Z-1$. By combining Eq. (B3) with Eq. (B4) and using Stirling's approximation to evaluate the logarithm of $Z!$, we obtain

$$\mu_{PP}/RT = \ln Z - \ln \nu_1 \tag{B5}$$

In order to calculate the value of ν_1, the number of ways of putting a single PP into a lattice containing N cubes, we employ the approximate counting method used by Shih and Alben[27] for a different lattice model (details of this calculation may be obtained from the present author). The final result is

$$\ln \nu_1 = \ln 6 + \ln M - f(\{a\},b,\phi) \tag{B6}$$

where ϕ is the volume fraction of cubes, Nb^3/M, and

$$f(\{a\},b,\phi) = -(a_1a_2a_3)\ln(1-\phi) + (a_1+a_2+a_3-3)\ln(1-\phi+\phi/b) + [a_1a_2+a_2a_3+a_1a_3-2(a_1+a_2+a_3)+3]\ln(1-\phi+\phi/b^2) + (a_1a_2a_3-a_1a_2-a_2a_3-a_1a_3+a_1+a_2+a_3-1)\ln(1-\phi+\phi/b^3)$$

Combining Eqs. (B5) and (B6), we obtain

$$\mu_{PP}/RT = -\ln 6 + \ln(Z/M) + f(\{a\},b,\phi) \quad \text{(B7)}$$

It may be readily shown that

$$\lim_{\phi\to 0} f(\{a\},b,\phi) = 0$$

Thus, $-\ln 6 + \ln Z/M$ may be identified as the ideal part of the chemical potential, μ_{PP}^{I} (note that Z/M is proportional to the volume concentration of PPs), and $f(\{a\},b,\phi)$ as the nonideal part, μ_{PP}^{NI}.

APPENDIX C

Comparison of the Results of Lattice and Scaled Particle Calculations of Activity Coefficients and Nonideal Free-Energy Changes

It was pointed out that because of an unrealistic simplification, the lattice model would be expected to underestimate the nonideal part of the chemical potential, and hence the activity coefficient, of a parallelopiped (PP) in an environment of cubes. We can obtain a quantitative measure of the degree to which these quantities are underestimated by calculating the value of μ_{PP}^{NI} ($\ln \gamma_{PP}$) for a cube of volume v in an environment of cubes of volume v_b using both the lattice model and the scaled particle theory. The results of this comparison are shown in Fig. C1, where the ratio of $\ln \gamma_{PP}$ calculated using the lattice model to that calculated using the scaled particle theory is plotted as a function of the ratio v_b/v for various values of ϕ, the volume fraction of cubes in the environment. As expected, the ratio $\ln \gamma_{PP}$(lattice)/$\ln \gamma_{PP}$(scaled particle) is less than unity under all conditions, but increases toward unity as the size of cubes in the environment increases relative to the size of the reference cube. The value of the ratio decreases sharply with increasing ϕ and is particularly low when ϕ is high and v_b/v is low.

Another comparison which is relevant to the present study is the calculation of the nonideal part of the free-energy change associated with a model self-association process. We represent this process by the replacement of n "reactant" cubes of volume v by a single "product" cube of volume nv. While the results for $n = 2$, 3, and 4 are not analytically equal, they differ only by 1–2%. As might be expected, the results are qualitatively similar

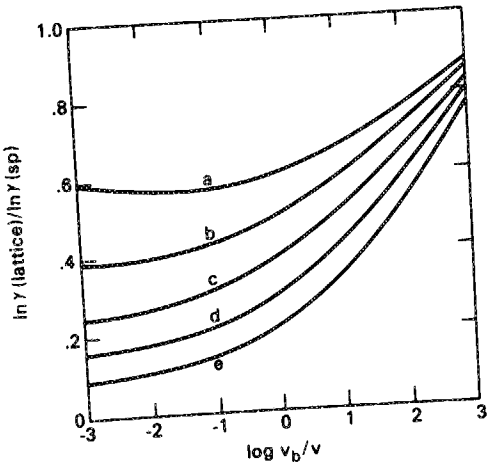

Fig. C1. Ratio of ln γ calculated using lattice model to that calculated using scaled particle theory, plotted as a function of the ratio of the volumes of background and reference particles. (a) $\phi = 0.1$; (b) $\phi = 0.2$; (c) $\phi = 0.3$; (d) $\phi = 0.4$; (e) $\phi = 0.5$.

to those obtained when calculating activity coefficients. The underestimate of ΔG^{NI} by the lattice model is most severe for high values of ϕ and for low values of v_b/v.

We may use the results presented above to scale up the estimates of activity coefficients and/or nonideal free-energy changes calculated using the lattice model, as shown in the following illustration. Let us, for example, calculate the activity coefficient of a PP of dimensions $S \times S \times 2S$ in an environment containing cubes of side S at a density $\phi = 0.3$. It will be assumed that the ratio of the value of ln γ_{PP} calculated from the lattice model to the "true" value of ln γ_{PP} is approximately equal to the ratio ln γ_{PP}(lattice)/ln γ_{PP}(scaled particle) for a cube with the same volume as the PP (side $2^{1/3}S$) in the same environment. From Fig. C1 we see that this ratio is about 0.45. Thus, the "true" value of ln γ_{PP} would be expected to be approximately 2.2 times as large as that calculated from the lattice model.

APPENDIX D

Dependence of Encounter Rate on ϕ

The rate at which molecules of substrate S and enzyme E encounter each other in solution is proportional to the sum of their respective coefficients of self-diffusion[28]:

$$\text{encounter rate} = k_e[\text{S}][\text{E}] \qquad \text{(D1)}$$

$$k_e \propto D_\text{S} + D_\text{E}$$

The self-diffusion coefficient of a macromolecule is dependent on the concentration of macromolecules in solution. For example, the logarithm

of the self-difffusion coefficient of hemoglobin decreases roughly linearly with hemoglobin concentration with a slope of approximately 1 decade/35 g/dl.[29] Qualitatively similar results are found in solutions of serum albumin.[30] A theoretical analysis[31] suggests that the observed dependence of diffusion coefficient on concentration in protein solutions at neutral pH and moderate ionic strength derives essentially entirely from the space-filling properties of the macromolecules and not from specific interactions between them. It follows that if a second macromolecular species were present in trace amounts in a solution of, say, hemoglobin, the self-diffusion coefficient of the second species would decrease in parallel with that of the hemoglobin with increasing hemoglobin concentration. We may thus write, as a rough approximation

$$D \simeq D^0 e^{-g\phi} \tag{D2}$$

where g is a constant whose magnitude depends on the relative sizes and shapes of the trace species and the predominant space-filling species. In a solution containing two trace species (enzyme E and substrate S), we may write

$$k_3 \propto D_S^0 e^{-g_S\phi} + D_E^0 e^{-g_E\phi} \tag{D3}$$

If S is a small molecule, it is likely that $D_S^0 \gg D_E^0$ and $g_S \ll g_E$. If S and E are macromolecules of similar size and shape, then $D_S^0 \simeq D_E^0$ and $g_S \simeq g_E$. In both cases, k_e may be approximated by an expression of the form of text Eq. (24).

I thank Drs. T. L. Hill and P. D. Ross for critically reading and commenting on the initial draft of this report.

References

1. Dittmer, D. S., Ed. (1961) *Blood and Other Body Fluids*, FASEB, Washington, D.C.
2. Skinner, G. B. (1974) *Introduction to Chemical Kinetics*, Academic Press, New York.
3. Ross, P. D. & Minton, A. P. (1977) *J. Mol. Biol.* **112**, 437–452.
4. Ross, P. D., Briehl, R. W. & Minton, A. P. (1978) *Biopolymers* **17**, 2285–2288.
5. Ross, P. D. & Minton, A. P. (1977) *Biochem. Biophys. Res. Commun.* **76**, 971–976.
6. Lebowitz, J. L., Helfand, E. & Praestgaard, E. (1965) *J. Chem. Phys.* **43**, 774–779.
7. Gibbons, R. M. (1969) *Mol. Phys.* **17**, 81–86.
8. Adams, E. T., Jr. & Fujita, H. (1963) in *Ultracentrifugal Analysis in Theory and Experiment*, Williams, J. W., Ed., Academic Press, New York, pp. 119–128.
9. Adams, E. T., Jr. (1965) *Biochemistry* **4**, 1655–1659.
10. Ogston, A. G. & Winzor, D. J. (1975) *J. Phys. Chem.* **79**, 2496–2500.
11. Nichol, L. W. & Winzor, D. J. (1976) *J. Phys. Chem.* **80**, 1980–1982.
12. Hill, T. L. & Chen, Y. (1973) *Biopolymers* **12**, 1285–1312.
13. Ross, P. D. & Minton, A. P. (1979) *Biochem. Biophys. Res. Commun.* **88**, 1308–1314.
14. Laurent, T. C. (1971) *Eur. J. Biochem.* **21**, 498–506.
15. Jancsik, V., Keleti, T., Nagy, M. Fenyvesi, E., Bartha, A., Rudas, A., Kovacs, P. & Wolfram, E. (1979) *J. Mol. Catalysis* **6**, 41–49.
16. Laurent, T. C. & Obrink, B. (1972) *Eur. J. Biochem.* **28**, 94–101.
17. Obrink, B. & Laurent, T. C. (1974) *Eur. J. Biochem.* **41**, 83–90.

18. Benesch, R. E., Benesch, R., Edalji, R. & Kwong, S. (1978) *Biochem. Biophys. Res. Commun.* **81,** 1307–1311.
19. Behe, M. & Englander, S. W. (1978) *Biophys. J.* **23,** 129–145.
20. Sunshine, H. R., Hofrichter, J. & Eaton, W. A. (1979) *J. Mol. Biol.* **133,** 435–467.
21. Wilf, J. & Minton, A. P. (1981) *Biochim. Biophys. Acta*, in press.
22. Hoagland, V. D. Jr. & Teller, D. C. (1969) *Biochemistry* **8,** 594–602.
23. Lakatos, S., Zavodszky, P. & Elödi, P. (1972) *FEBS Lett.* **20,** 324–326.
24. Minton, A. P. & Wilf, J. (1981) *Biochemistry*, in press.
25. Gibbons, R. M. (1970) *Mol. Phys.* **18,** 809–816.
26. Flory, P. J. (1953) *Principles of Polymer Chemistry*, Cornell U. P., Ithaca.
27. Shih, C.-S. & Alben, R. (1972) *J. Chem. Phys.* **57,** 3055–3061.
28. Gutfreund, H. (1972) *Enzymes: Physical Principles*, Wiley-Interscience, London.
29. Gros, G. (1978) *Biophys. J.* **22,** 453–468.
30. Keller, K. H., Canales, E. R. & Yum, S. I. (1971) *J. Phys. Chem.* **75,** 379–387.
31. Minton, A. P. & Ross, P. D. (1978) *J. Phys. Chem.* **82,** 1934–1938.

Received April 24, 1980
Accepted March 4, 1981